ACS SyntheticBiology

Letter

pubs.acs.org/synthbio

Feedback Control of Protein Expression in Mammalian Cells by Tunable Synthetic Translational Inhibition

James A. Stapleton,[†] Kei Endo,[‡] Yoshihiko Fujita,[†,‡] Karin Hayashi,[‡] Masahiro Takinoue,[§] Hirohide Saito,[‡,∥,⊥,*] and Tan Inoue[†,‡,*]

[†]Laboratory of Gene Biodynamics, Graduate School of Biostudies, Kyoto University, Oiwake-cho, Kitashirakawa, Sakyo-ku, Kyoto 606-8502, Japan

[‡]International Cooperative Research Project, Japan Science and Technology Agency, 5 Sanban-cho, Chiyoda-ku, Tokyo 102-0075, Japan

[§]Department of Computational Intelligence and Systems Science, Interdisciplinary Graduate School of Science and Engineering, Tokyo Institute of Technology, Yokohama, Kanagawa 226-8503, Japan

[∥]The Hakubi Center, Kyoto University, Oiwake-cho, Kitashirakawa, Sakyo-ku, Kyoto 606-8502, Japan

[⊥]Center for iPS Cell Research and Application, Kyoto University, 53 Kawahara-cho, Shogoin, Sakyo-ku, Kyoto 606-8507, Japan

Supporting Information

ABSTRACT: Feedback regulation plays a crucial role in dynamic gene expression in nature, but synthetic translational feedback systems have yet to be demonstrated. Here we use an RNA/protein interaction-based synthetic translational switch to create a feedback system that tightly controls the expression of proteins of interest in mammalian cells. Feedback is mediated by modified ribosomal L7Ae proteins, which bind a set of RNA motifs with a range of affinities. We designed these motifs into L7Ae-encoding mRNA. Newly translated L7Ae binds its own mRNA, inhibiting further translation. This inhibition tightly feedback-regulates the concentration of L7Ae and any fusion partner of interest. A mathematical model predicts system behavior as a function of RNA/protein affinity. We further demonstrate that the L7Ae protein can simultaneously and tunably regulate the expression of multiple proteins of interest by binding RNA control motifs built into each mRNA, allowing control over the coordinated expression of protein networks.

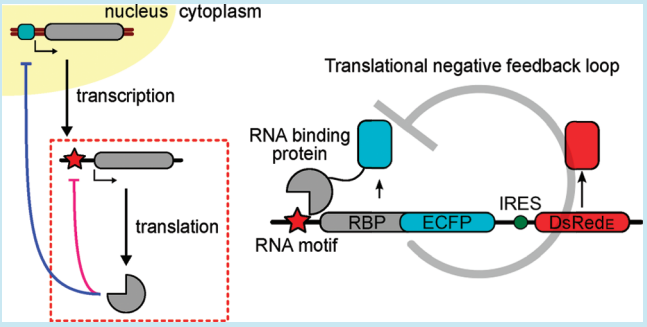

KEYWORDS: *synthetic biology, feedback, translational regulation, RNA, L7Ae, RNA−protein interactions*

The ability to robustly and tunably control protein expression is central to the continued progress of molecular bioengineering. Historically, techniques for recombinant protein production have focused on maximizing overexpression, but today the advancing complexity of synthetic gene networks demands the optimization of complex pathways composed of multiple proteins. Limited options are available in any host organism for controlling protein concentrations. In mammalian cell systems, recent work has dramatically expanded the transgene expression control toolbox,[1−9] allowing researchers to begin to assemble simple synthetic parts into complex devices such as synthetic band-detect networks and oscillators. However, despite the significant progress, the shortage of parts to enable quantitative control of protein expression remains especially acute in mammalian systems.

Feedback regulation is ubiquitous in biology and fundamental to many engineering applications. Synthetic biologists have designed and characterized a wide range of engineered biological transcriptional feedback regulation systems.[10,11] Negative and positive transcriptional feedback has been used to stabilize desired output protein concentrations,[12] accelerate system dynamics,[13] and generate biological oscillations.[14−17] Less work has been done to this point to characterize translational feedback systems, which are potentially superior to transcriptional systems when a stable, optimal output concentration is desired.[18,19] In nature, translational inhibition feedback loops are common in both prokaryotes and eukaryotes. For instance, ribosomal and other RNA-binding proteins often repress their own translation by binding their encoding mRNAs at sites that mimic their functional targets. Examples include the L30 protein,[20] the S15 protein,[21] and the U1A protein.[22] Mimicking this natural role of RNA−protein (RNP) interactions in a synthetic translational feedback control system is a promising strategy for regulating protein expression in mammalian cells.

RNA-based synthetic biology tools[23−25] are a natural fit for translational control systems, and synthetic RNA-based systems

Received: September 7, 2011
Published: November 30, 2011

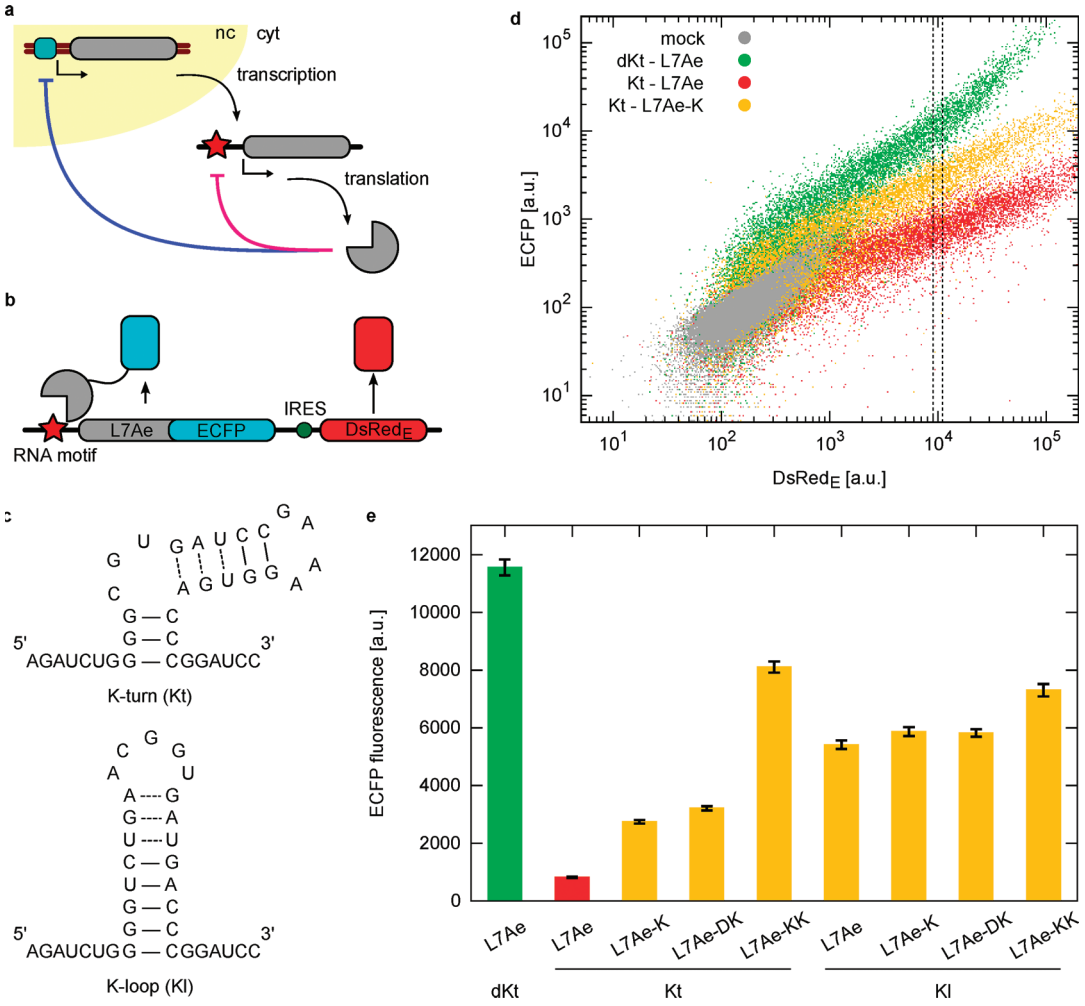

Figure 1. The strength of the RNP interaction determines the level of protein expression *via* translational regulation. (a) Translational regulation creates a tighter feedback loop than transcriptional feedback, in which protein synthesis continues from existing mRNA. nc: nucleus; cyt: cytoplasm. (b) Schematic diagram of the feedback repression construct. An IRES allowed the translation of a second fluorescent reporter protein, DsRed$_E$, to proceed unaffected by L7Ae repression. (c) Comparison of the secondary structures of the K-turn and K-loop motifs. (d) Log–log FACS dot plot showing ECFP and DsRed$_E$ fluorescence intensities of cells transfected with feedback plasmids encoding indicated RNA motif/protein pairs. Mock-transfected cells are shown in gray. Plots of the other tested RNP pairs are shown in Supplementary Figure S4. (e) Average ECFP fluorescence intensity for cells with DsRed$_E$ fluorescence near the arbitrarily chosen value 10^4 (dotted lines shown in panel d). Lower values indicate stronger feedback repression. Error bars indicate standard error of the mean (SEM), where n = 216, 311, 266, 279, 398, 298, 284, 301, and 380 cells, respectively. Kt: K-turn; Kl: K-loop; dKt: a defective K-turn with no affinity for L7Ae. Representative data from one of four independent experiments are shown.

have been successfully demonstrated in mammalian cells.[6,7,26−34] RNP-mediated synthetic translational systems that take advantage of natural translational control mechanisms have also been constructed in mammalian cells. In one system, translation of a target mRNA was regulated by specific binding of the CNBP and La proteins to designed sequences engineered into the 5′ untranslated region.[35] However, none of these systems have been demonstrated in a feedback configuration.

Previously we described a synthetic switch in which an RNA binding protein represses the translation of a target mRNA.[33] The switch exploits the ribosomal protein L7Ae of *Archaeoglobus fulgidus*, which binds tightly to the K-turn RNA motif.[36] This motif was incorporated into the target mRNA upstream of the open reading frame. The resulting tight association between the L7Ae protein and the mRNA effectively repressed translation. This translational repression system has been successfully linked to output phenotypes such as cell fate.[34]

In this work, we demonstrate the first synthetic translational feedback regulatory system. An L7Ae fusion protein regulates the translation of its own mRNA (Figure 1a and b) in HeLa human cervical cancer cells. The resulting feedback-enforced fusion protein concentration can be tuned by substituting mutants of the L7Ae protein and the K-turn RNA sequence to adjust the strength of the RNA/protein interaction. By mixing and matching RNP pairs, biological engineers can choose the feedback repression strength (and the corresponding target protein concentration) optimal for each application.

The protein-mediated translational regulation of our previous system is ideal for constructing synthetic feedback loops.[33] However, while the binary ON/OFF behavior that results from the tight binding of L7Ae to the K-turn motif makes an excellent switch, the strong repression limits the adaptability of the system to other applications, including feedback. To tune the strength of the translational inhibition, we replaced the L7Ae protein, the K-turn RNA motif, or both with variants that

dx.doi.org/10.1021/sb200005w | *ACS Synth. Biol.* 2012, 1, 83−88

Table 1. Surface Plasmon Resonance Measurements of Binding Constants[a] and In-Cell Measurements of Pseudo Binding Constants (κ) between L7Ae Variants and RNA Motifs

	K-turn				K-loop			
	k_{on} [/Ms]	k_{off} [/s]	K_D [M]	κ	k_{on} [/Ms]	k_{off} [/s]	K_D [M]	κ
L7Ae	4.5×10^5 $\pm 3.4 \times 10^3$	7.1×10^{-4} $\pm 4.7 \times 10^{-5}$	1.6×10^{-9} (1.6 nM)	4.6×10^1	8.0×10^5 $\pm 3.8 \times 10^3$	1.8×10^{-3} $\pm 4.5 \times 10^{-5}$	2.2×10^{-9} (2.2 nM)	4.2×10^3
L7Ae-K	1.4×10^5 ± 830	2.0×10^{-3} $\pm 3.7 \times 10^{-5}$	1.5×10^{-8} (15 nM)	7.6×10^2	2.7×10^5 ± 810	7.0×10^{-3} $\pm 2.7 \times 10^{-5}$	2.6×10^{-8} (26 nM)	5.9×10^3
L7Ae-DK	2.8×10^5 ± 890	6.5×10^{-3} $\pm 2.8 \times 10^{-5}$	2.4×10^{-8} (24 nM)	1.1×10^3	5.2×10^5 $\pm 5.1 \times 10^3$	0.028 $\pm 3.4 \times 10^{-4}$	5.4×10^{-8} (54 nM)	6.1×10^3
L7Ae-KK	4.8×10^4 ± 340	0.033 $\pm 2.2 \times 10^{-4}$	6.8×10^{-7} (680 nM)	9.7×10^3	7.9×10^4 $\pm 1.4 \times 10^3$	0.17 $\pm 1.6 \times 10^{-3}$	2.2×10^{-6} (2200 nM)	1.0×10^4

[a]The parameter set from one of three independent analyses is shown. Response curves are provided as Supplementary Figures S2 and S3.

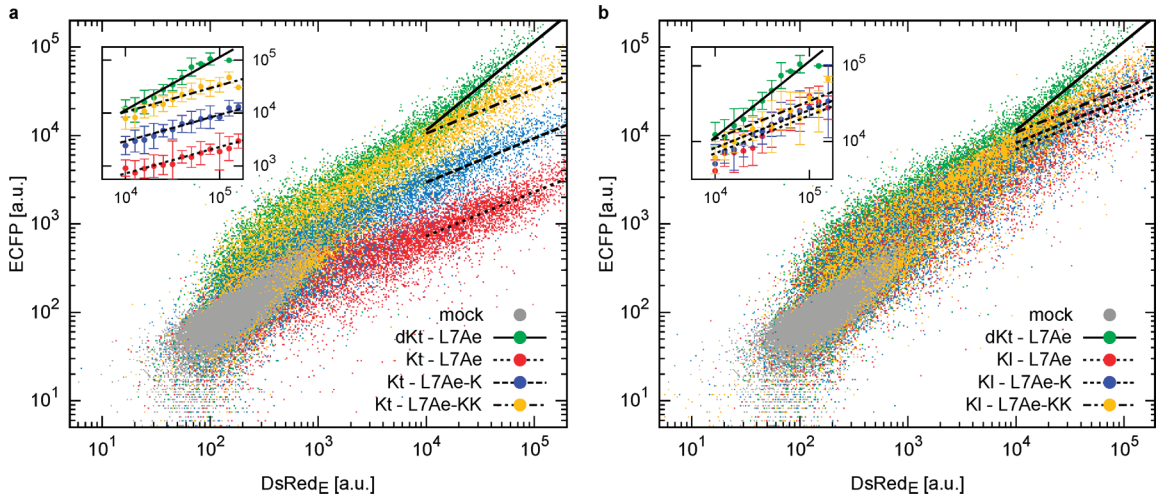

Figure 2. A mathematical model fit to FACS data. Green dots: no feedback; orange dots: L7Ae-KK; blue dots: L7Ae-K; red dots: L7Ae; gray dots: mock transfection. Four lines indicate the fitting results of the model. Insets show the fitting results along with measured average ECFP fluorescences; error bars indicate the standard deviation. (a) K-turn construct data. (b) K-loop construct data.

bound with weaker affinity. In place of L7Ae, we substituted L7Ae-K37A (referred to here as L7Ae-K), L7Ae-D54A-K79A (L7Ae-DK), and L7Ae-K37A-K79A (L7Ae-KK), mutants containing amino acid changes predicted to affect RNA binding from analysis of the cocrystal structure[37] and from high degrees of conservation in a sequence alignment (Supplementary Figure S1). As an alternative to the K-turn RNA motif we employed the K-loop, a related motif that forms a kinked structure similar to the K-turn but binds less tightly to L7Ae.[38]

We measured the *in vitro* binding characteristics of each RNA-protein pair by surface plasmon resonance (Table 1 and Supplementary Figures S2 and S3). The on rate, off rate, and dissociation constant (K_D) varied among the different combinations of L7Ae mutants and RNA motifs. As expected, the wild-type L7Ae/K-turn pair, which caused strong translational repression in our previous report, bound with the tightest affinity, and the measured K_D of 1.6 nM was consistent with previously published measurements.[33,39,40] The K_D of the protein/RNA permutations ranged from 1.6 nM to 2.2 μM.

We then tested the strength of the *in vivo* feedback repression that resulted from each protein/RNA pair. To construct feedback control elements, we inserted an RNA motif (K-turn, K-loop, or a nonfunctional RNA motif) upstream of an open reading frame encoding the L7Ae protein (or one of its variants) fused to a model protein of interest, enhanced cyan fluorescent protein (L7Ae-ECFP) (Figure 1b). In this configuration, the translated fusion protein should feedback-inhibit the synthesis of additional copies of itself by binding to its encoding mRNA. An internal ribosome entry site (IRES) on the same mRNA allowed the translation of a second fluorescent reporter protein, DsRed-Express (DsRed$_E$), to proceed unaffected by L7Ae repression (Figure 1b). Fluorescence-activated cell sorting (FACS) of transfected HeLa cells revealed that the repression strengths of the alternate binding pairs fell between the strong repression of the wild-type L7Ae/K-turn interaction (Figure 1d and e, red) and the absence of repression (Figure 1d and e, green, measured using a K-turn mutant with no affinity for L7Ae). Repression strength generally increased with increasing binding strength (decreasing *in vitro* K_D, Figure 1e and Supplementary Figure S4). In cells harboring strong feedback repression plasmids, ECFP fluorescence was lowered by more than an order of magnitude.

To describe the behavior of the feedback repression system, we derived a mathematical model:

$$\frac{dx}{dt} = \alpha_{DsRed} c_{mRNA} - \lambda_{DsRed} x$$
$$\frac{dy}{dt} = \frac{\alpha_{CFP} c_{mRNA}}{(1 + y/K)^n} - \lambda_{CFP} y \quad (1)$$

where variables x and y and constant c_{mRNA} indicate the concentrations of DsRed$_E$, L7Ae-ECFP, and mRNA, respectively; α_{DsRed} and α_{CFP} are the synthesis rates of DsRed$_E$ and L7Ae-ECFP from mRNA; and λ_{DsRed} and λ_{CFP} are their

dx.doi.org/10.1021/sb200005w | *ACS Synth. Biol.* 2012, 1, 83–88

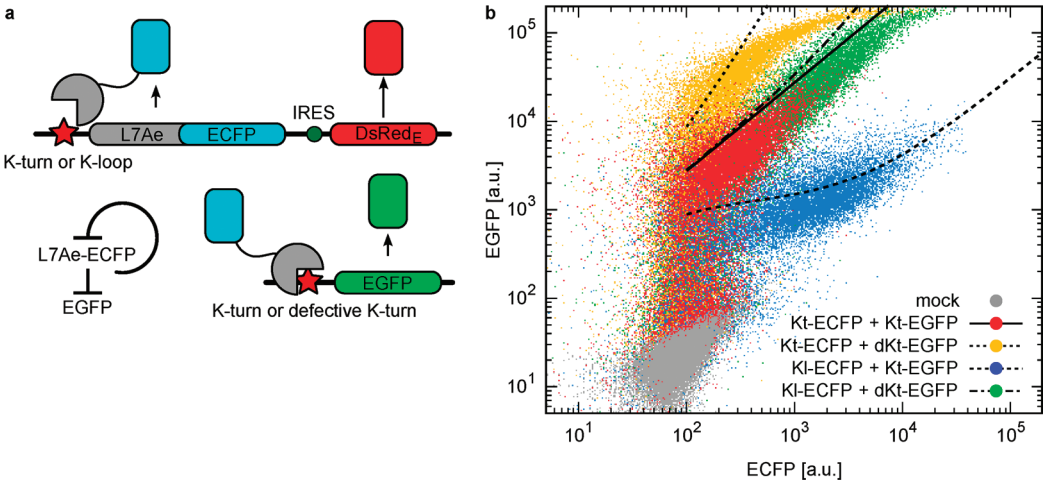

Figure 3. An L7Ae-ECFP control protein simultaneously regulates two transcripts with different RNA motifs. (a) L7Ae-ECFP simultaneously regulates its own expression by feedback in *cis* and the expression of EGFP in *trans*. (b) FACS dot plot overlaid with the prediction from the model. The four populations (identified in the panel) form the corners of a square, with high (dKt) or low (Kt) EGFP fluorescence and intermediate (Kl) or low (Kt) ECFP fluorescence. Representative data from one of four independent experiments are shown. The predicted behaviors of ECFP and EGFP fluorescence for each construct are consistent with the experimental data.

degradation rates. K indicates the dissociation constant between L7Ae-ECFP (or its mutants) and an RNA motif (K-turn or K-loop). The coefficient n is defined such that $n = 1$ in the case of negative feedback regulation of the synthesis of L7Ae-ECFP, and $n = 0$ when there is no feedback. From a steady-state assumption ($dx/dt = dy/dt = 0$), we have the following equation:

$$X = \gamma Y\left(1 + \frac{Y}{\kappa}\right)^n \tag{2}$$

where X and Y are the experimentally observed fluorescence data for DsRed$_E$ and L7Ae-ECFP; κ is a pseudo dissociation constant; and γ is a constant (see Supporting Information for the full derivation and explanation).

By fitting the K-turn construct data shown in Figure 1e and Supplementary Figure S4 to eq 2 (Figure 2a), the pseudo dissociation constant κ was obtained as $\kappa = 4.6 \times 10^1$ (L7Ae), 7.6×10^2 (L7Ae-K), 1.1×10^3 (L7Ae-DK), and 9.7×10^3 (L7Ae-KK) (Table 1). In the data fitting, we used only those points with high DsRed$_E$ values (above 10^4), in accordance with an assumption of the model (see eqs S3 and S4 in Supporting Information). These *in vivo* constants increase with each mutation, in agreement with the corresponding *in vitro* dissociation constants (Table 1, K-turn). For the K-loop constructs (Figure 2b), we obtained $\kappa = 4.2 \times 10^3$ (L7Ae), 5.9×10^3 (L7Ae-K), 6.1×10^3 (L7Ae-DK), and 1.0×10^4 (L7Ae-KK). This trend did not match well the corresponding *in vitro* dissociation constants for K-loop (Table 1, K-loop). The discrepancy may result from weaker affinity between K-loop and L7Ae in the cellular environment compared to *in vitro*; our system may prove to be an effective way to measure RNP affinity within cells.

We next constructed a system in which a single control protein (L7Ae-ECFP) simultaneously regulated the expression of multiple target proteins within the same cell. We cotransfected HeLa cells with a plasmid encoding the enhanced green fluorescent protein (EGFP) behind a K-turn or defective K-turn motif in addition to one of the feedback plasmids (Figure 3a). In the resulting system, L7Ae-ECFP binds to its own mRNA and controls its own concentration *in cis* while simultaneously regulating *in trans* the translation of a second protein of interest, EGFP. FACS analysis confirmed that the fluorescent reporters were simultaneously repressed at levels that corresponded to the strength of the respective RNA-protein interactions (Figure 3b).

To predict the behavior of this complex system, we extended the mathematical model by adding the following equation to eq 1:

$$\frac{dw}{dt} = \frac{\alpha_{GFP} c'_{mRNA}}{(1 + y/K')^{n'}} - \lambda_{GFP} w \tag{3}$$

where w and c'_{mRNA} indicate the concentrations of EGFP and EGFP-coding mRNA; α_{GFP} and λ_{GFP} are synthesis and degradation rates of EGFP; and K' is the dissociation constant between L7Ae-ECFP (or its mutants) and a second (K-turn or defective K-turn) RNA motif. The coefficient n' is defined such that $n' = 1$ in the case of *in trans* repressive regulation of the synthesis of EGFP, and $n' = 0$ when there is no regulation. Applying the steady-state assumption to eqs 1 and 3, and using the experimentally obtained values for the pseudo dissociation constant κ derived from Figure 2, we were able to correctly predict the behavior of the system (Figure 3b, black lines) (see Supporting Information for the full calculations). Additionally, we refit the κ parameters using only the data shown in Figure 3 in order to evaluate our prediction (see Supporting Information for the full calculations). The resulting values of the pseudo dissociation constant κ (for feedback) and κ' (for L7Ae-ECFP binding to the second reporter mRNA) were quite similar to those of κ obtained from the single feedback configuration (Supplementary Table 1), indicating that parameters obtained from our simpler system are valid and sufficient to predict the function of a more complex system. The predictability observed here reaffirms that while purely *in vitro* analysis is not sufficient to predict system behavior in cells (κ values for K-loop in Table 1 and Figure 2b), complex regulation systems can be modeled using experimentally obtained parameters. The agreement of the results with simple mathematical models implies that the system is orthogonal to cellular pathways and is not disrupted by unknown factors.

dx.doi.org/10.1021/sb200005w | *ACS Synth. Biol.* 2012, 1, 83–88

The result of Figure 3 confirms that a single L7Ae protein can simultaneously control the concentrations of multiple genes at different levels by interacting with RNA motifs of different binding affinities. Expression levels can be adjusted globally by the choice of L7Ae variant or individually by the choice of the RNA motif. The strong L7Ae/K-turn binding pair and natural homologues provide a starting point for the creation of a collection of intermediate-affinity mutants. Replacing the RNA motifs used in this study with an aptamer sequence that binds a protein of interest could simplify the system by removing the requirement for an L7Ae protein fusion.[6]

A recent report[19] described a synthetic incoherent feed-forward system that stabilizes a steady-state output level against variations in the amount of DNA template. In the system, post-transcriptional feed-forward regulation was achieved by employing synthetic microRNAs (miRNA). The performance of the feed-forward system matched the predictions of a model and was comparable to the performance of our system. An advantage of the miRNA system is the specificity of RNAi, which should facilitate the simultaneous regulation of multiple outputs with different miRNAs. While it may be possible to tune the strength of the feed-forward system by using miRNAs with different RNAi potencies, fine-tuning was not attempted in the report. An advantage of our system is the direct protein-mediated feedback regulation, which allows a protein of interest expressed in cells to rapidly and tunably regulate its own expression levels and those of multiple additional outputs.

Our regulatory system is triggered by a protein (rather than a small molecule) and controls translation (rather than transcription). These unusual features enable direct translational feedback and render the system orthogonal to and easily integrated with traditional control systems. Such integration is common in nature, where the simultaneous control of transcription and translation is frequently used to fine-tune protein levels.[41,42] Beyond serving as a useful synthetic biology tool, we anticipate that the system described here will prove useful in the study of natural regulation, just as synthetic circuits have been used to study natural biological circuits.[43]

METHODS

Protein and RNA Preparation. Proteins were expressed and purified as previously described.[33] Further purification was performed on a HiTrap Heparin HP column using an ÄKTA explorer system (GE Healthcare, Little Chalfont, U.K.). Detailed methods are provided in the Supporting Information. DNA templates for *in vitro* transcription were generated by primer extension reaction with ExTaq (TaKaRa Bio, Otsu, Japan) and purified with phenol-chloroform extraction and ethanol precipitation. RNA fragments were transcribed *in vitro* using MEGAshortscript (Ambion, Austin, TX), purified by denaturing PAGE, and recovered from the gel slices. The transcripts were then extracted with phenol-chloroform, precipitated with ethanol, and washed by ultrafiltration using Microcon YM-10 (Millipore, Billerica, MA).

Surface Plasmon Resonance. SPR analysis was carried out in binding buffer containing 5% glycerol, 2 mM DTT, and 0.01% Tween-20 at 25 °C using a BIAcore 3000 instrument (GE Healthcare, Little Chalfont, U.K.). Proteins were immobilized on the sensor chip CM5 *via* amine coupling according to the manufacturer's instructions. RNA solutions were prepared in the same buffer, denatured at 96 °C for 5 min, refolded at room temperature, and serially diluted. Thirty microliters of each RNA solution was injected onto the sensor chip at a flow rate of 20 μL/min. The surface of the sensor chip was regenerated by an injection of 0.1 N NaOH for 5 s and equilibrated with the buffer before the next RNA injection.

Cell Culture. HeLa cells (0.5×10^5 per well) established in 24-well plates were cultured at 37 °C in a 1:1 mixture of Dulbecco's Modified Eagle Medium (DMEM) and nutrient mixture F-12 (Invitrogen, Carlsbad, CA). The media were supplemented with 10% (v/v) FBS and an antibiotic/antimycotic solution (A5955, Sigma Aldrich, St. Louis, MO). The incubator atmosphere was enriched with 5% CO_2. Cells were established in multiwell plates. After 1 day, the 70−80% confluent cells were transfected with plasmids (1 μg) using 1 μL of Lipofectamine 2000 (Invitrogen, Carlsbad, CA) following the manufacturer's instructions. Media were changed 4 h after transfection. For Figure 3b, cells were cotransfected with two plasmids (each 0.5 μg) using 1 μL of Lipofectamine 2000.

Fluorescence-Activated Cell Sorting (FACS). Twenty-four hours after transfection, HeLa cells were collected by trypsinization and resuspension in 200 μL of DMEM/F12 media. A total of 30,000 cells per sample were analyzed by fluorescence-activated cell sorting with a FACS Aria (BD Biosciences, San Jose, CA); 408 and 488 nm semiconductor lasers were used for excitation; and 450/40 nm, 530/30 nm, and 695/40 nm emission filters were used for ECFP, EGFP, and $DsRed_E$, respectively. Spectral overlaps were compensated using the FACS Diva software. Dead cells were excluded by gating out events with low FSC and SSC signals.

ASSOCIATED CONTENT

Supporting Information

Detailed derivation of the mathematical model, additional figures, and detailed methods. This material is available free of charge *via* the Internet at http://pubs.acs.org.

AUTHOR INFORMATION

Corresponding Author

*E-mail: saitou.hirohide.8a@kyoto-u.ac.jp, tan@kuchem.kyoto-u.ac.jp.

Author Contributions

J.A.S., K.E., Y.F., H.S., and T.I. designed the experiments. J.A.S., K.E., and K.H. performed the experiments. J.A.S., K.E., Y.F., M.T., H.S., and T.I. analyzed the data. J.A.S., K.E., Y.F., M.T., H.S., and T.I. wrote the manuscript.

Notes

The authors declare no competing financial interest.

ACKNOWLEDGMENTS

The authors thank T. Hara (Kyoto University) and A. Kitamura (ICORP, JST) for identifying the attenuated L7Ae mutants. We also thank A. Huttenhofer (Innsbruck Medical University, Biocenter) and T. S. Rozhdestvensky (University of Muenster) for providing the L7Ae plasmid. This work was supported by the International Cooperative Research Project (ICORP), JST. A part of this work was supported by a grant from the Takeda Science Foundation and the New Energy and Industrial Technology Development Organization (NEDO, 09A02021a) (H.S.). J.A.S. was supported by a Short-term Postdoctoral Fellowship from the Japan Society for the Promotion of Science.

REFERENCES

(1) Greber, D., and Fussenegger, M. (2007) Mammalian synthetic biology: engineering of sophisticated gene networks. *J. Biotechnol. 130*, 329−345.

(2) Nissim, L., and Bar-Ziv, R. H. (2010) A tunable dual-promoter integrator for targeting of cancer cells. *Mol. Syst. Biol. 6*, 1−10.

(3) Kramer, B. P., Viretta, A. U., Daoud-El-Baba, M., Aubel, D., Weber, W., and Fussenegger, M. (2004) An engineered epigenetic transgene switch in mammalian cells. *Nat. Biotechnol. 22*, 867−870.

(4) Kramer, B. P., and Fussenegger, M. (2005) Hysteresis in a synthetic mammalian gene network. *Proc. Natl. Acad. Sci. U.S.A. 102*, 9517−9522.

(5) Weber, W., Stelling, J., Rimann, M., Keller, B., Daoud-El-Baba, M., Weber, C. C., Aubel, D., and Fussenegger, M. (2007) A synthetic time-delay circuit in mammalian cells and mice. *Proc. Natl. Acad. Sci. U.S.A. 104*, 2643−2648.

(6) Culler, S. J., Hoff, K. G., and Smolke, C. D. (2010) Reprogramming cellular behavior with RNA controllers responsive to endogenous proteins. *Science 330*, 1251−1255.

(7) Chen, Y. Y., Jensen, M. C., and Smolke, C. D. (2010) Genetic control of mammalian T-cell proliferation with synthetic RNA regulatory systems. *Proc. Natl. Acad. Sci. U.S.A. 107*, 1−6.

(8) Leisner, M., Bleris, L., Lohmueller, J., Xie, Z., and Benenson, Y. (2010) Rationally designed logic integration of regulatory signals in mammalian cells. *Nat. Nanotechnol. 5*, 666−670.

(9) Weber, W., and Fussenegger, M. (2011) Molecular diversity—the toolbox for synthetic gene switches and networks. *Curr. Opin. Chem. Biol. 15*, 414−420.

(10) Andrianantoandro, E., Basu, S., Karig, D. K., and Weiss, R. (2006) Synthetic biology: new engineering rules for an emerging discipline. *Mol. Syst. Biol. 2*, 1−14.

(11) Mukherji, S., and Oudenaarden, A. van. (2009) Synthetic biology: understanding biological design from synthetic circuits. *Nat. Rev. Genet. 10*, 859−871.

(12) Becskei, A., and Serrano, L. (2000) Engineering stability in gene networks by autoregulation. *Nature 405*, 590−593.

(13) Rosenfeld, N., Elowitz, M. B., and Alon, U. (2002) Negative autoregulation speeds the response times of transcription networks. *J. Mol. Biol. 323*, 785−793.

(14) Elowitz, M. B., and Leibler, S. (2000) A synthetic oscillatory network of transcriptional regulators. *Nature 403*, 335−338.

(15) Stricker, J., Cookson, S., Bennett, M. R., Mather, W. H., Tsimring, L. S., and Hasty, J. (2008) A fast, robust and tunable synthetic gene oscillator. *Nature 456*, 516−519.

(16) Atkinson, M. R., Savageau, M. A., Myers, J. T., and Ninfa, A. J. (2003) Development of genetic circuitry exhibiting toggle switch or oscillatory behavior in *Escherichia coli*. *Cell 113*, 597−607.

(17) Tigges, M., Marquez-Lago, T. T., Stelling, J., and Fussenegger, M. (2009) A tunable synthetic mammalian oscillator. *Nature 457*, 309−312.

(18) Swain, P. S. (2004) Efficient attenuation of stochasticity in gene expression through post-transcriptional control. *J. Mol. Biol. 344*, 965−976.

(19) Bleris, L., Xie, Z., Glass, D., Adadey, A., Sontag, E., and Benenson, Y. (2011) Synthetic incoherent feedforward circuits show adaptation to the amount of their genetic template. *Mol. Syst. Biol. 7*, 519.

(20) Dabeva, M. D., and Warner, J. R. (1993) Ribosomal protein L32 of *Saccharomyces cerevisiae* regulates both splicing and translation of its own transcript. *J. Biol. Chem. 268*, 19669−19674.

(21) Philippe, C., Eyermann, F., Bénard, L., Portier, C., Ehresmann, B., and Ehresmann, C. (1993) Ribosomal protein S15 from *Escherichia coli* modulates its own translation by trapping the ribosome on the mRNA initiation loading site. *Proc. Natl. Acad. Sci. U.S.A. 90*, 4394−4398.

(22) Boelens, W. C., Jansen, E. J., van Venrooij, W. J., Stripecke, R., Mattaj, I. W., and Gunderson, S. I. (1993) The human U1 snRNP-specific U1A protein inhibits polyadenylation of its own pre-mRNA. *Cell 72*, 881−892.

(23) Saito, H., and Inoue, T. (2009) Synthetic biology with RNA motifs. *Int. J. Biochem. Cell Biol. 41*, 398−404.

(24) Wieland, M., and Fussenegger, M. (2010) Ligand-dependent regulatory RNA parts for Synthetic Biology in eukaryotes. *Curr. Opin. Biotechnol. 21*, 760−765.

(25) Liang, J. C., Bloom, R. J., and Smolke, C. D. (2011) Engineering biological systems with synthetic RNA molecules. *Mol. Cell 43*, 915−926.

(26) Isaacs, F. J., Dwyer, D. J., Ding, C., Pervouchine, D. D., Cantor, C. R., and Collins, J. J. (2004) Engineered riboregulators enable post-transcriptional control of gene expression. *Nat. Biotechnol. 22*, 841−847.

(27) Deans, T. L., Cantor, C. R., and Collins, J. J. (2007) A tunable genetic switch based on RNAi and repressor proteins for regulating gene expression in mammalian cells. *Cell 130*, 363−372.

(28) Rinaudo, K., Bleris, L., Maddamsetti, R., Subramanian, S., Weiss, R., and Benenson, Y. (2007) A universal RNAi-based logic evaluator that operates in mammalian cells. *Nat. Biotechnol. 25*, 795−801.

(29) Beisel, C. L., Bayer, T. S., Hoff, K. G., and Smolke, C. D. (2008) Model-guided design of ligand-regulated RNAi for programmable control of gene expression. *Mol. Syst. Biol. 4*, 224.

(30) An, C.-I., Trinh, V. B., and Yokobayashi, Y. (2006) Artificial control of gene expression in mammalian cells by modulating RNA interference through aptamer-small molecule interaction. *RNA 12*, 710−716.

(31) Babiskin, A. H., and Smolke, C. D. (2011) A synthetic library of RNA control modules for predictable tuning of gene expression in yeast. *Mol. Syst. Biol. 7*, 471.

(32) Win, M. N., and Smolke, C. D. (2007) A modular and extensible RNA-based gene-regulatory platform for engineering cellular function. *Proc. Natl. Acad. Sci. U.S.A. 104*, 14283−14288.

(33) Saito, H., Kobayashi, T., Hara, T., Fujita, Y., Hayashi, K., Furushima, R., and Inoue, T. (2010) Synthetic translational regulation by an L7Ae-kink-turn RNP switch. *Nat. Chem. Biol. 6*, 71−78.

(34) Saito, H., Fujita, Y., Kashida, S., Hayashi, K., and Inoue, T. (2011) Synthetic human cell fate regulation by protein-driven RNA switches. *Nat. Commun. 2*, 160.

(35) Schlatter, S., and Fussenegger, M. (2003) Novel CNBP- and La-based translation control systems for mammalian cells. *Biotechnol. Bioeng. 81*, 1−12.

(36) Klein, D. J., Schmeing, T. M., Moore, P. B., and Steitz, T. A. (2001) The kink-turn: a new RNA secondary structure motif. *EMBO J. 20*, 4214−4221.

(37) Moore, T., Zhang, Y., Fenley, M. O., and Li, H. (2004) Molecular basis of box C/D RNA-protein interactions; cocrystal structure of archaeal L7Ae and a box C/D RNA. *Structure 12*, 807−818.

(38) Gagnon, K. T., Zhang, X., Qu, G., Biswas, S., Suryadi, J., Brown, B. A., and Maxwell, E. S. (2010) Signature amino acids enable the archaeal L7Ae box C/D RNP core protein to recognize and bind the K-loop RNA motif. *RNA 16*, 79−90.

(39) Turner, B., Melcher, S. E., Wilson, T. J., Norman, D. G., and Lilley, D. M. J. (2005) Induced fit of RNA on binding the L7Ae protein to the kink-turn motif. *RNA 11*, 1192−1200.

(40) Rozhdestvensky, T. S., Tang, T. H., Tchirkova, I. V., Brosius, J., Bachellerie, J. P., and Huttenhofer, A. (2003) Binding of L7Ae protein to the K-turn of archaeal snoRNAs: a shared RNA binding motif for C/D and H/ACA box snoRNAs in Archaea. *Nucleic Acids Res. 31*, 869−877.

(41) Saklatvala, J., Dean, J., and Clark, A. (2003) Control of the expression of inflammatory response genes. *Biochem. Soc. Symp. 70*, 95−106.

(42) Lal, A., Abdelmohsen, K., Pullmann, R., Kawai, T., Galban, S., Yang, X., Brewer, G., and Gorospe, M. (2006) Posttranscriptional derepression of GADD45alpha by genotoxic stress. *Mol. Cell 22*, 117−128.

(43) Sprinzak, D., and Elowitz, M. B. (2005) Reconstruction of genetic circuits. *Nature 438*, 443−448.